REPORT DOCUMENTATION PAGE

Form Approved
OMB No. 0704-0188

PLEASE DO NOT RETURN YOUR FORM TO THE ABOVE ADDRESS.

1. REPORT DATE *(DD-MM-YYYY)*	2. REPORT TYPE	3. DATES COVERED *(From - To)*
13 JULY 2012	Final Technical	01 APR 2009 - 31 MAR 2012

4. TITLE AND SUBTITLE

UNMANNED AERIAL SYSTEMS (UAS) MISSION PLANNING

5a. CONTRACT NUMBER

5b. GRANT NUMBER

FA9550-09-1-0271

5c. PROGRAM ELEMENT NUMBER

6. AUTHOR(S)

Kurt Barnhart

5d. PROJECT NUMBER

5e. TASK NUMBER

5f. WORK UNIT NUMBER

7. PERFORMING ORGANIZATION NAME(S) AND ADDRESS(ES)

Kansas State University

8. PERFORMING ORGANIZATION REPORT NUMBER

9. SPONSORING/MONITORING AGENCY NAME(S) AND ADDRESS(ES)

AFOSR
875 N. Randolph St
Arlington, VA 22203
Dr. Willard Larkin/RSL

10. SPONSOR/MONITOR'S ACRONYM(S)

11. SPONSOR/MONITOR'S REPORT NUMBER(S)

AFRL-OSR-VA-TR-2012-1060

12. DISTRIBUTION/AVAILABILITY STATEMENT

Distribution A: Approved for Public Release

13. SUPPLEMENTARY NOTES

14. ABSTRACT

The objectives of this award has been achieved and exceeded. The objective was to establish and initialize UAS operational protocols and procedures to incorporate UAS training and test capability within Kansas in conjunction with the Kansas national guard. This award has enabled follow-on funding which has resulted in UAS operational capability using multiple UAS platforms in support of multiple missions including workforce training as well as payload and airspace integration testing in addition to routine operations. This funding has allowed Kansas State University to establish itself as an international leader in this technical area and has contributed to state and local economic development initiatives.

15. SUBJECT TERMS

16. SECURITY CLASSIFICATION OF:			17. LIMITATION OF ABSTRACT	18. NUMBER OF PAGES	19a. NAME OF RESPONSIBLE PERSON
a. REPORT	b. ABSTRACT	c. THIS PAGE			Kurt Barnhardt
unclassified	unclassified	unclassified	unclassified (U)		19b. TELEPHONE NUMBER *(Include area code)* kurtb@k-state.edu

To: AFOSR Technical Reports

From: R. Kurt Barnhart, Ph.D. Principle Investigator

Date: July 3, 2012

Subject: Final Report for Report Titled: Unmanned Aerial Systems (UAS) Mission Planning

Abstract: The objectives of this award has been achieved and exceeded. The objective was to establish and initialize UAS operational protocols and procedures to incorporate UAS training and test capability within Kansas in conjunction with the Kansas National Guard. This award has enabled follow-on funding which has resulted in UAS operational capability using multiple UAS platforms in support of multiple missions including workforce training as well as payload and airspace integration testing in addition to routine operations. This funding has allowed Kansas State University to establish itself as an international leader in this technical area and has contributed to state and local economic development initiatives. This project and the follow-on project

I. *Kansas State University at Salina*
Advanced Aviation Research Center
2011/2 AFOSR Report

Airspace Integration

List of current AARC COAs for Airspace (NAS) Access:

- **Pending**:

  2012-CSA-11-COA Submitted: 1/23/12, Validated: N/A, Location: SLN, Airframe: Crow, Type: Initial

  2012-CSA-24-COA Submitted: 3/6/12, Validated: N/A, Location: MHK, Airframe: SpyKat, Type: Initial

- **Approved:**

2011-CSA-31-COA Submitted: 04/31/11, Approved: 07/12/11, Location: CCTC, Airframe: Wolverine III Type: Initial

2011-CSA-33-COA Submitted: 04/27/11, Approved: 07/12/11, Location: CCTC, Airframe: Aerosonde Mk4.7, Type: Initial

2011-CSA-51-COA Submitted: 06/21/11, Approved: 08/12/11, Location: KSLN, Airframe: Aerosonde Mk4.7, Type: Initial

2011-CSA-83-COA Submitted: 12/06/11, Approved: 02/15/12, Location: CCTC, Airframe: Crow, Type: Initial

2012-CSA-1-COA Submitted: 01/11/12, Approved: 03/12/12, Location: CCTC, Airframe: Willie, Type: Initial

- **Draft:**

  1. Airframe: Penguin B, Location: CCTC, Type: Initial

Student Training/Airspace Integration

During the summer of 2011 the KSU UAS department finalized its training syllabus and UAV training fleet. The current structure for NAS integration for UAS student training utilized our COA strategy along with the Air National Guard's Smokey Hill Bombing range.

KSU UAS students start their training on simulation mission scenarios that were created to integrate them into multiple aspects of flight planning with regards to NAS integration. Through review of the mission log files the students learn where possible conflicts may arise from improper planning of such things as lost-link way points of emergency operations. These mission scenarios are premised around domestic operations involving UAS.

The UAS flight training utilizes a step graduating structure in UAV complexity. After the students have acquired the needed procedural skills through the simulation they progress to actual UAV flights. The students first learn how to operate within the Certificate of Authorization and how to activate through proper SOPs. Starting with the Wolverine III UAV, students learn how to operate a very rudimentary VTOL UAS. After training completion on the Wolverine III they progress to the Crow UAV. The Crow UAS is a basic hand-launch/belly recovery system without ISR capabilities. Students are taught the basic skills in operating a sophisticated GCS while adapting to longer range mission planning. The next phase of flight training utilizes the Penguin B UAV. The same sophisticated GCS is used as the Crow however the students are adapted to Auto-Takeoff and Landing procedures. In the Penguin B training students also start applying their CRM

through working with the Sensor operator and Crew Chief. The student's final process in their training is operating the Aerosonde Mk4.7 UAV. During this final phase students are taught alternate methods of Launch and Recovery elements such as catapult, vehicle, and net. The mission planning and integration knowledge becomes imperative at this phase due to the long duration, long distance, and de-confliction needed during these missions. The Aerosonde training is conducted in three sub-stage locations. The first stage is conducted at the Crisis City location where students apply de-confliction tactics, search technics, and in-depth CRM processes. The second stage is conducted in R-3601 Smoky Hill bombing range. Here the students apply long flight duration tactics, airspace de-confliction, and long range operations. The final stage is conducted at the Salina Class D airport. The students launch the Aerosonde from an active class D airport and into a deconflicted traffic pattern where the UA is then joined by a manned chase aircraft. The students will then start the UA toward the loiter area located 5NM away over the Crisis City training area. During this operation the student does a GCS handoff to another GCS and PIC located at Crisis City. The Aerosonde can then be recovered at the Crisis City runway or return to Salina via the chase aircraft and recover. During this training structure, students are trained in all aspects of UAS operations. The students train with classmates in different positions such as Safety Officer, PIC, Sensor operator, Maintenance, and Crew chief. The Sensor operator is trained in the operations of EO/IR gimbaled cameras as related to domestic ops.

Through this student training KSU is gathering data on many different aspects of UAS flight in the NAS and how manned processes can be adopted. One of the next phases of our NAS integration research will be focused on the fusion of FAA NextGen technology/airspace and UAS.

KSU UAS Assets Procured (2011) with AFOSR Funding

Aerosonde Mk 4.7(E) UAS platform from AAI (a Textron Company):

- The Aerosonde is a fixed wing aircraft capable of launch and recovery from most any road, runway (improved and non-improved), or field. The aircraft can be launched off the top of a vehicle accelerating to 45 MPH. This newer model will be catapult launched and recovered by belly landing.
- It is a versatile and proven platform with hundreds of thousands of flight hours in theater.
- Aircraft is currently equipped with a TASE Duo gimbal payload incorporating both EO and IR cameras.
- The aircraft has been integrated with the world's smallest Mode C transponder. KSU has teamed with Sagetech Inc and is testing the first experimental unit and follow up TSO'd Mode S with ADS-B capabilities.
- The aircraft will be used for Airspace Integration, UAS Avionics Research, Student training and Search and Rescue.
- The aircraft is equipped with a C-Band analog video transmitter that can be received by any L3 ROVER system. This transmitter is planned to upgrade to a digital S or L band with more capabilities.
- Capabilities:

- 18 hour flight duration
- ~ 8 mile operating distance on 900MHz (can be indefinite if upgraded to KU-Band).
- 8 pounds of payload
- 17,000’ service ceiling
- ~ 45 minute setup time to launch

Two Penguin B UAS from UAV Factory:

- Fixed wing UAS Platforms
- The Penguin B is has an unleaded fuel 2-stroke with long endurance capabilities.
- The Penguins will be used for student training, airspace integration research, and Search and Rescue in the State.
- KSU is currently modifying a gimbaled digital camera system that conducts it’s communications via network protocol (IEEE 802.11)
- Capabilities:
  - 10 hours with reserve flight duration
  - 7 miles
  - 12 pound payload
  - 20 minute setup time to launch
  - 15000’ + operating altitude

Fixed-wing UAS, the Crow from KSU:

- Fixed-wing electric UAS platform and all supporting equipment
- This is a fixed-wing UAS platform from a modified electric RC platform.
- The APV-4 will be used for airspace integration research (specifically class D UAS operations), and student training.
- Specs:
  - Cruise Speed –35 MPH
  - Ceiling –10,000 ft
  - Wingspan –6.5 ft
  - Weight –12 lbs
  - Payload –2 lbs
  - Flight Duration-30 hrs

Piccolo UAS Autopilot system from Cloud Cap Technology:

- UAS Autopilot, Ground Control Station and supporting Software
- This autopilot system is top of the line and gives KSU – Salina the ability to fly both fixed wing or rotor wing UAVs.
- Currently one of the Piccolo systems is integrated into our new Aerosonde 4.7.
- Two more Piccolo systems are integrated into Crow platforms. These platforms are being used for student education regarding how to initially setup UAS autopilots, conduct Hardware in the Loop simulations, map gains files, and integrate the systems as a whole.
- This autopilot uses 900Mhz or KU band satellite for C2
- We will also be integrating a FreeWave OEM board radio for 2C2 capability.

Staffing:

UAS Pilot/Instructor
A full time UAS Pilot/Instructor was hired to be primarily responsible for UAS flight operations and procedures. They perform a variety of complex tasks in the design, development, qualification, modification, troubleshooting, integration, and testing of prototypes. Their duties require them to serves as a member of the UAS Pilot and/or Sensor operator for evaluation, operational, and research flight tests; As well as Pilot/Sensor instruction in lab and/or classroom environment. This person also provide daily safety evaluations of associated flight assets and procedures; Develops and executes standard operating procedures for UAS flights.

Bio's:

Dr. Kurt Barnhart – Aviation Department Head

Dr. Barnhart is Professor and Head of the Aviation Department at Kansas State University in addition to serving as the executive director of the Applied Aviation Research Center which oversees the newly established Unmanned Aerial Systems program office. Dr. Barnhart is a member of the graduate faculty at K-State and holds a commercial pilot certificate with instrument, multi-engine, seaplane and glider ratings. He also is a certified flight instructor with instrument and multi-engine ratings. Dr. Barnhart also holds an airframe and powerplant certificate with inspection authorization. Dr. Barnhart holds an A.S. in Aviation Maintenance Technology from Vincennes University, a B.S. in aviation administration from Purdue University, an MBAA from Embry-Riddle Aeronautical University, and a Ph.D. in educational administration from Indiana State University. Dr Barnhart's Research agenda is focused in aviation psychology and Human Factors. His industry experience includes work as a R&D inspector with Rolls Royce Engine Company, and systems instructor for American Trans-Air airlines. Most Recently Dr. Barnhart was an Associate Professor and Acting Department Chair of the Aerospace Technology at Indiana State University where he was responsible for teaching flight and upper division administrative classes. Dr. Barnhart is an invited speaker at Bombardier's international Safety Standdown in Kansas.

Josh Brungardt – UAS Program Director

Josh Brungardt has served as the Chief Pilot for High Performance Aircraft Training, EFIS Training, and Lancair Aircraft. He currently is serving as the Unmanned Aircraft System (UAS) Director for Kansas State University's Aviation department. Brungardt also holds the UAS chair for the Kansas Aviation Advisory Committee. In 2010 Josh attended Senior Officer training on the Predator UAS at Creech AFB with the 11th

Reconnaissance SQ. In addition to completing over 100 first flights on experimental aircraft he has served as a test pilot and instructor pilot to the U.S. Air Force. He also specializes in Electronic Flight Information Systems (EFIS) and avionics integration. In 2006 Brungardt started a pilot training company called EFIS Training, which focused on pilots transitioning to glass cockpits. He holds ATP & CFII ratings with over 4000 hours, as well as having raced at the Reno National Air Races. Brungardt received a bachelor's degree in airway science and an associate's degree in professional pilot from Kansas State at Salina.

Eric Shappee – UAS Lead Professor

Eric Shappee serves as an associate professor of aviation at Kansas State University at Salina in the professional pilot program. Professor Shappee teaches numerous aviation course to include: Introduction to Aviation, System Safety, Safety Management, and Introduction to Unmanned Aerial Systems. He holds a commercial pilot certificate with instrument, multi-engine, and glider ratings. He is also a certified flight instructor with gold seal. Professor Eric Shappee holds two Associate Degrees from Antelope Valley College, a Bachelors in Aeronautical Science and a Master in Aeronautical Science and Safety from Embry-Riddle Aeronautical University. Professor Shappee's main area of focus in aviation is safety. He has developed several risk assessment tools for the University and other aviation organizations. Further, he was named as a member of the International Society of Air Safety Investigators, a membership earned through professional service and experience. Professor Shappee has been active in the field of aviation since 1986 and teaching since 1995. During his career in aviation, professor Shappee has also spent time working with unmanned aerial systems including the Predator, and Aerosonde.

Richard Brown – UAS Technician

Richard Brown is a FAA certificated private pilot as well as a certified airframe & powerplant technician. Brown has worked as an aircraft maintenance technician in the corporate, airline, and heavy maintenance environments. He is maintenance certified on numerous sUAS including the Aerosonde Mk 4.7 and Wolverine III platforms. Richard is also a proficient RC aircraft pilot and UAS External pilot. He has earned a bachelor's Degree in Aviation Management, and associate's Degree Aircraft Maintenance.

Kirk Demuth – UAS Pilot

Kirk M. Demuth graduated from Kansas State University in Salina in May of 2007 with degrees in Aviation and Technology. After graduation, Kirk served as chief pilot and maintenance director for Chalk 2 Aviation in Victorville, CA, where he accumulated more than 1,000 hours of unmanned aerial vehicle formation flying as a chase plane

observer for the Predator and Reaper military unmanned aerial vehicles. In 2009, Kirk returned to Kansas State University to head up the newly established Unmanned Aircraft Systems Program Office. There, he was trained on the Aerosonde UAS and worked with industry to help with the safe integration of UAS in the National Airspace System. At K-State, Kirk worked closely with Flint Hills Solutions, a high technology UAS company, on the evaluation of UAS applications for emergency response. In 2010, he took a position at Flint Hills Solutions as Vice President of UAS operations. Now, after over two years of intensive research and development and flight testing of unmanned helicopter systems, Kirk has returned to Kansas State University to assist in future research and development and student UAS instruction.

II. Wireless Power Transmission System

Saeed Khan, Nathan Maresch, Justin Kuntz

One of the potential ways to improve the endurance of small electronic remotely piloted vehicles (RPV) is to charge their batteries on the fly by wirelessly beaming radio frequency (RF) power to them. Two basic methods are under consideration. The first involves a focused microwave beam to transfer the power. The second method, of which we have focused our efforts, employs antennas operating at a much lower frequency than microwaves. This method, designed for the high frequency (HF) band is to operate in the near field, with only small losses due to radiated (far field) power. This type of wireless power transmission (WPT) system has been shown to be capable of transferring power in a highly efficient manner, especially when the receiving antenna is in close proximity of the transmitting antenna.

Either of the WPT systems would have an air or ground based transmitting system rapidly transferring energy to the RPV in order to cause as little mission disruption as possible. Functional areas for the HF WPT system include (a) a highly efficient rectenna system including antennas and power conversion circuits, (b) a power management system capable of rapid charging, (c) a charging platform, and (d) a cooling system for the transmitting unit. Our preference thus far has been the selection of a ground-based mobile platform to house the transmitting unit, which contains a number of components including a signal generator and multiple amplifier stages.

The receiving section includes an antenna system with rectifier, and a hardware-based power management system. For testing

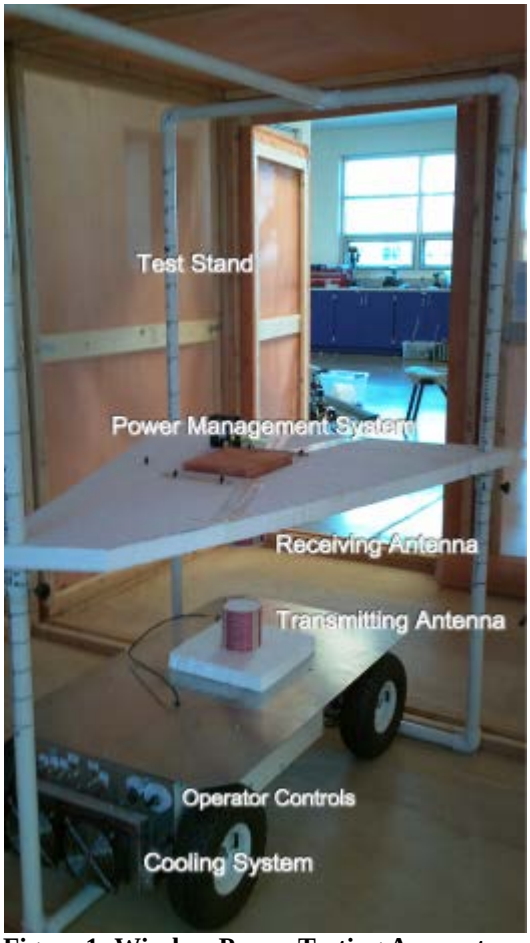

Figure 1: Wireless Power Testing Apparatus

purposes, the receiving unit is placed on an adjustable stand placed over the transmitting element. When fielded, the receiving section could potentially be placed in an appropriate mobile unit (such as a quad-copter) that can be positioned on or near the top of the platform to be charged through wireless power coupling.

The ultimate future realization would be a miniaturization and repackaging of the transmitting apparatus into an RPV of sufficient size in order for it to act as a tanker unit –recharging smaller electric units on the fly as required (with regulatory approval). While early demonstrations show very good power transfer when antennas are in close proximity, moderate efficiencies may be possible to several feet.

Faraday Cage

For testing of the wireless power transmission system, a modular faraday cage with a footprint of approximately twelve feet by eight feet was constructed to keep the high frequency RF energy localized within. The shielding material consists of copper mesh with 100 wires per inch (100 Mesh). Common building materials were used for the construction of each panel frame. On each edge that contacts another panel, a gasket-like material was included under the mesh to provide a tight seal at each connection point. Each panel is secured to the next via bolts inside. An RF power entrance filter is included to prevent conducted signals from passing along the power cable as it transitions inside the cage. The door is sealed tightly from the outside using spring-loaded latches. The cage was tested by placing a signal source inside, while testing outside using a spectrum analyzer. Significant savings resulted from constructing a faraday cage using

Figure 2: Faraday cage with WPT signal generation cart with platform removed

relatively inexpensive materials versus purchasing a commercial model.

Transmitter Cart Platform

An RF power generation apparatus was built, consisting of a signal source followed by a number of amplifier stages in order to achieve the goal of supplying 100 watts of

continuous power. RF filters are included at the signal generator, as well as on the final output line to reduce harmonics. The output filter has a number of selection settings for the particular HF passband desired. Infrared remote capability was added to the unit to enable basic operation through the faraday cage.

All of the electronic components were assembled onto a backplane. This backplane installs into a small mobile cart, which may be used as a landing platform. The platform can be easily removed to reveal the components inside the cart as shown in Figure 3. Operator controls are mounted on the rear panel of the cart, just above the cooling system (Figure 1).

Figure 3: RF Transmitter Electronics Installed in Mobile Cart

Antenna Simulation/Prototyping

Simulations were key in determining the feasibility of different sizes and geometries of antennas for use with wireless power transmission. A coiled helical antenna design was chosen for both the transmitting and receiving antennas, which are tuned to operate at or near the high frequency ISM (Industrial, Scientific, Medical) band of 13.56 MHz. Antenna element design was initially based on an overall coiled wire dipole length of 1/2 wave, and then lengthened/shortened based on simulation and/or test results. Simulations were performed using both the 4nec2, and CST Microstripes software packages. The latest antenna prototype, shown in

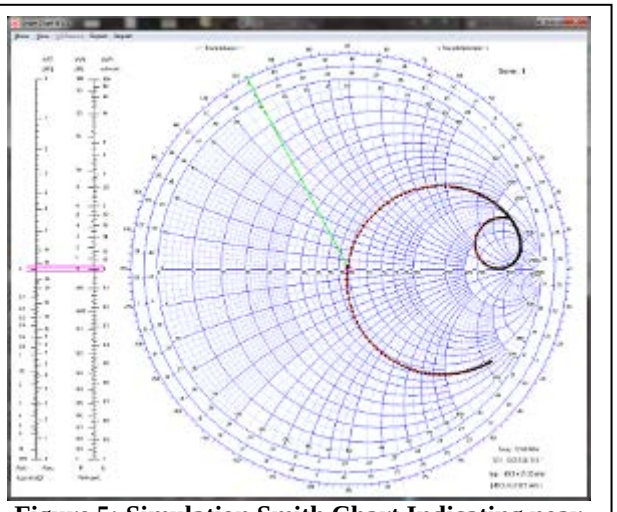

Figure 5: Simulation Smith Chart Indicating near perfect match at 12.68 MHz for 15 cm distance

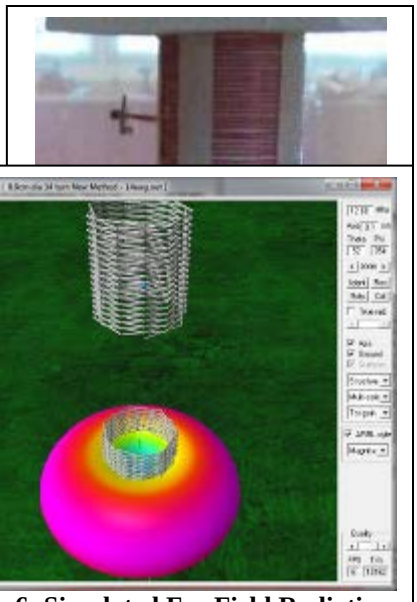

Figure 6: Simulated Far Field Radiation Pattern (Best Gain -30dBi)

figure 4, is constructed of 34 turns of 14-awg wire. For a 15 cm gap between antenna elements, the 4nec2 simulations indicated a very good impedance match at 12.68 MHz (very little reflected signal as shown in figure 5), and a very poor far field radiation pattern as indicated in Figure 6. This suggests near-field coupling of the energy.

Power Management System

A power management circuit was constructed to rapidly receive and store incoming wireless power. The circuit contains ultracapacitors, which are rapidly able to store incoming power due to their high power density. They are able to deliver and receive power much faster than a rechargeable battery; however, most batteries have a higher energy density than ultracapacitors, meaning they are capable of storing more overall energy. As a result, the power management system contains both technologies. Once the capacitors are full, a circuit begins fast charging a NiMh battery, transitioning to a trickle charge once full. Both the ultracapacitors and the battery power the load. In this way, the circuit utilizes the major benefits of both energy storage technologies, offering a reasonable balance between energy density for supplying the load, and power density for fast recharge. In the event that the ultracapacitors become fully discharged, the system includes a circuit that disengages the ultracapacitors; thus preventing the series battery from reverse charging the capacitors as current continues to flow. Allowing the capacitors to fully discharge is a significant benefit, as their full capacity may be utilized. Though the discharge current is limited, the capacitors can be rapidly recharged independently of the battery.

Figure 7: 25 Farad Ultracapacitors

Similar to most modern battery chemistries, ultracapacitors require balancing if placed in series. This prevents the overcharging of one or more individual capacitors in a series string, which would cause a failure due to the breakdown of the dielectric material. Balancing, therefore adds extra circuitry, and with it inefficiencies, which could be avoided if the capacitors were placed in parallel. For this reason, and due to the fact that capacitors add when in parallel, the prototype initially used a bank of parallel capacitors in series with a battery. Initial testing resulted in longer than expected charging times. This was due to the RC time constant, as the DC resistance of the circuit (only about 0.3 ohms) significantly contributes. Assuming 100 Farads of capacitance (4 parallel 25F Capacitors) results in an expected charging time of over two minutes; therefore, future designs must use series capacitors with balancing circuitry, or some series/parallel combination.

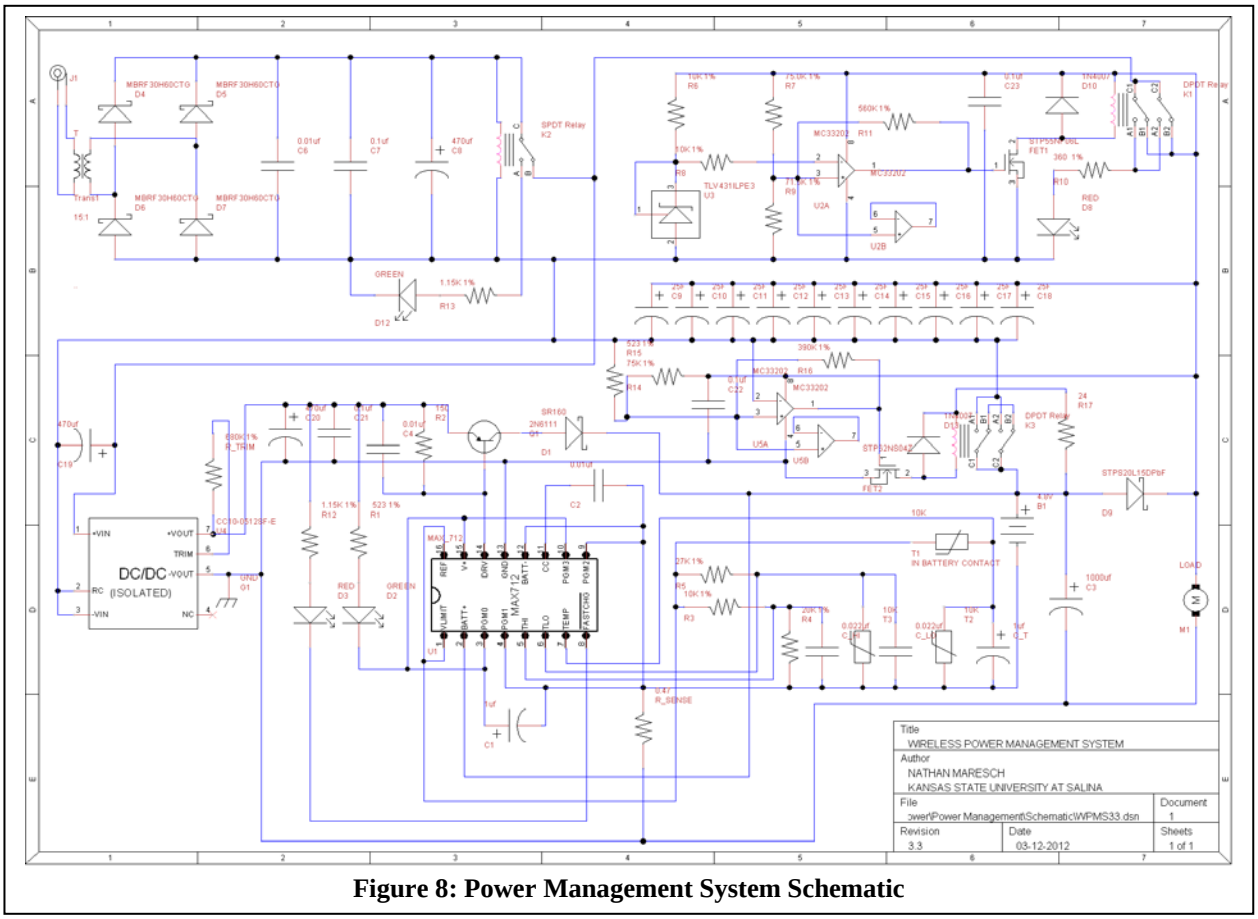

Figure 8: Power Management System Schematic

Testing/Results

For testing purposes, the transmitting antenna element is mounted on the cart platform, and an adjustable test stand supports the receiving antenna and power management circuitry (Figure 1). Antenna elements were initially checked using the two-port insertion loss (S21) measurement feature on the network analyzer. The antennas were placed on the test stand, spaced at specific distances apart. Each measurement indicated an optimum frequency at which the least signal loss between the antenna elements occurred. Without further tuning, the optimum frequency for a distance of 15 cm is 12.81 MHz. Though slightly higher in frequency, this coincides quite well with the 12.68 MHz value obtained through simulation. As seen in Figure 9, the insertion loss for a 15 cm distance is -1.72 dB, which indicates that more than 67% of the test signal was collected at the receiving port of the network analyzer.

34 Turn 14-Awg Tests			
Frequency MHz	**S11 dB**	**S21 dB**	**Dist. Of Separation cm**
12.00	-16.7	-0.98	5
12.62	-19.1	-1.26	10
12.81	**-14.0**	**-1.72**	**15**
12.91	-7.9	-2.85	20
12.94	-4.3	-6.60	30
12.94	-3.5	-10.60	40
12.94	-3.0	-16.0	60

Figure 9: Network Analyzer S-Parameter Measurements

For wireless power testing, all tests are

performed with the hardware sealed within the faraday cage. The wireless power transmission system is activated in a reduced power mode via an infrared remote from outside the faraday cage. After a predetermined amount of run time elapses, the system is powered down and the ultracapacitor voltage is immediately checked to determine the amount of energy wirelessly received and stored. From data we have accumulated so far, a series capacitor bank (of two capacitors) was able to charge to about the same percentage of its maximum capacity in about the same amount of time as a single capacitor (~60% in 20 sec.).

While still in the early stages, initial tests of the wireless power transmission system indicate promising results. Though we used helical antennas, other antenna topologies may prove superior for wireless power transfer overall. In addition, power management circuits may benefit from using slightly modified strategies for efficiently receiving and storing wireless power.

Conjugate Heat Transfer for Wireless Power Amplifier

Matthew J. Williamson, P.E., Dr. Saeed M. Khan, Justin Kuntz

Introduction

Wireless power transfer is a technology quickly expanding in application. One such application is the use of wireless power technology on remote platforms. Advances in this area will allow electronic devices to be powered without human presence in difficult locations, including harsh climates.
This study explores the use of a forced-air system combined with a commercially available amplifier and heat sink. The design modeled was selected based on simplicity and availability of materials.

Methodology

This study modeled a heat sink, which was already affixed to a wireless power amplifier, and available commercially. Other parts of the model were constructed to match the forced-air cooling system that was built from readily available and easy-to-use materials. One-eighth inch thick galvanized steel created a simple duct system through which electronic fans move air at varying ambient temperatures. Additionally, the model utilizes a boundary heat source, inlet and exit conditions for flowing air, and ambient temperatures to predict the temperature profile and maximum temperatures of the heat sink during operation. Variables considered include ambient temperature, inlet air velocity, and thermal conductivity of the heat sink. These variations will be compared to experimental data to determine the relative accuracy of each model. The maximum temperature predicted by the model will determine the velocity of forced-air required to maintain a stable working temperature for the wireless power amplifier, specifically in a hot environment. Solutions that limit the maximum temperature at the heat sink to 150 degrees F are sought. This limit will allow for stable operation of the amplifiers semiconductors.

Use of COMSOL Multiphysics

This study utilizes the Conjugate Heat Transfer physics, from the Heat Transfer Module, within COMSOL Multiphysics. Parts included in the model are representative of real parts used in the study, and are geometrically accurate. Materials used include 6000-series aluminum, galvanized steel, and air. Material properties for aluminum and air are directly from the software's material library. Appropriate material properties for the galvanized steel ductwork were added from these references:
[http://www.thermoworks.com, as of July 2011.] and
[http://www.galvanizeit.org/aga/designing-fabricating/design-considerations/zinc-metal-properties, as of July 2011.].

The variable ambient temperature of the model was used as an initial condition. At the interface of the amplifier and heat sink, a boundary heat source was applied as a boundary condition. A conservative assumption was made that the entire 200W rated

output of the device would be applied at this boundary. Varying model types applied the output power over the entire surface of the heat sink, or concentrated at specific amplifier to-heat sink connections. Boundary conditions were applied at the inlet of the adjacent duct so that the air was being received at the ambient temperature, and with a known inlet velocity. Another boundary condition allowed for air to outlet at standard atmospheric pressure.

Three model combinations were utilized in this study. The first model assumes that heat from the amplifier is evenly distributed over the top surface of the heat sink, and that the heat sink has a constant thermal conductivity, k, equal to 217 (W/m*K). The second model maintains the distributed heat assumption, but utilizes a temperature-dependent function for the thermal conductivity of aluminum. This temperature dependent function was derived from a reference table [http://www.efunda.com/materials/elements/TC_Table.cfm?Element_ID=al, as of July 2011.]. For temperatures ranging from 300 to 600K, a function in the third order of temperature fit the reference values with an R2 of 0.9995. The relationship of this temperature dependent function to the referenced data is found in Figure 1. Model 3 concentrates the boundary heat to six specific locations to mimic the connections made between the actual amplifier and heat sink. Figures 2 and 3 give a visual representation of the temperature distribution for the differing model types. Temperatures range from the ambient temperature input to the predicted maximum surface temperature. The very distinct differences between uniformly distributed and concentrated boundary heat sources are shown in the two figures.

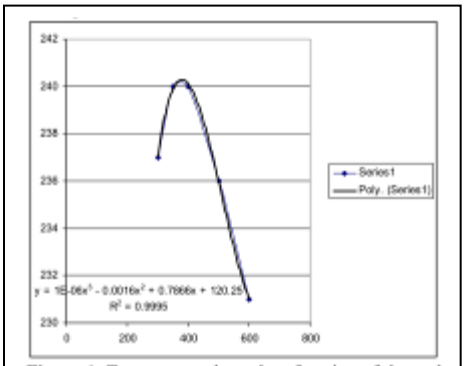

Figure 1. Temperature-dependant function of thermal conductivity of aluminum.

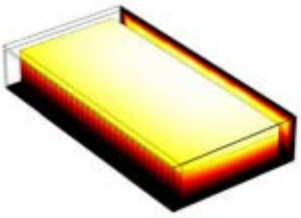
Figure 2. Temperature distribution for uniformly distributed heat source.

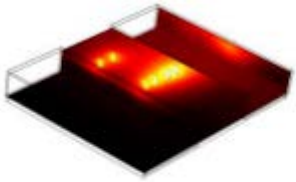
Figure 3. Temperature distribution for concentrated heat source.

Figure 4 compares the resulting maximum temperatures predicted by each model, using an ambient temperature of 130F over a range of inlet air velocities. This ambient temperature was selected as a very high, but realistically achievable temperature. Figure 4 relates the maximum temperature achieved on the surface of the heat sink for all three models at varying inlet air velocities. The data shows little variation in maximum temperatures between the constant and temperature-dependent thermal conductivity values, Models 1 and 2. The greatest variation is found when the boundary heat

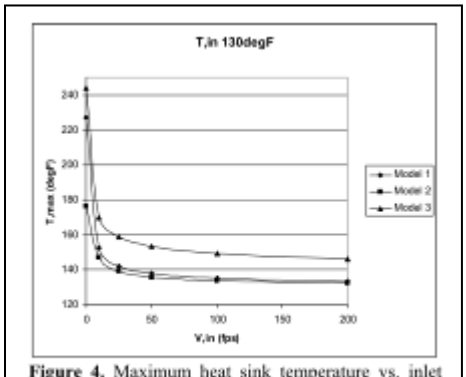

Figure 4. Maximum heat sink temperature vs. inlet velocity for three model assumptions with ambient temperature of 130 degrees F.

source condition is changed from the uniform distribution to the six concentrated locations of Model 3.

Model 3 proved to be the most conservative of the three models tested at 130 degrees F. Further modeling was completed to show variations in performance of this model over a range of ambient temperatures. This data can be seen in Figure 5. Of particular interest here, is where each predicted curve passes the 150 degree F threshold. With ambient temperatures up to 115 degrees F, cooling the heat sink requires relatively little airflow.

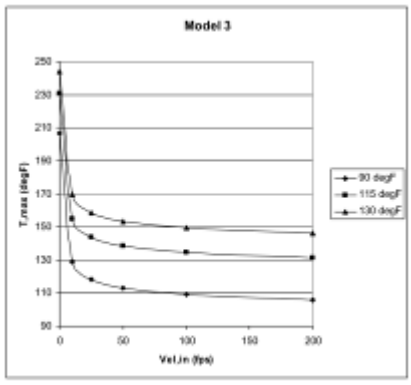

Figure 5. Maximum heat sink temperature vs. inlet velocity for three ambient temperatures.

In addition to the thermal conduction of each material, the radiation of both metals was considered. The "radiate-to-ambient" boundary condition was applied to all exterior aluminum and galvanized steel boundaries. The ambient temperature to which the metals radiate is the same variable temperature at the air inlet.

This study was undertaken to better understand the thermal management performance of a commercially available amplifier and heat sink system. Using COMSOL multiphysics software to model a real forced-air solution, several conclusions can be made.

First, for operation at high temperature, some cooling system is required. When airflow across the heat sink approached zero, maximum temperatures on the heat sink were significantly greater than those at which the amplifier would be stable. This was found true for all model types.

The inlet velocity needed to maintain a stable environment varied with ambient temperature and model assumptions. Model 3, with concentrated boundary heat sources, were consistently the most conservative. In order to maintain heat sink temperatures at or below 150 degrees F in a 130 degree F ambient environment, Model 3 required an inlet air velocity of 100 feet per second. Lower ambient temperatures and less conservative models all required significantly less airflow.

Future considerations include collecting experimental data for the modeled system. This data will be used to confirm the accuracy of the modeled system. Additionally, more novel cooling systems will be considered. Goals will include reducing the weight and power needs of the entire thermal management system.

In addition to this 200W amplifier, a 2kW wireless power amplifier solution has been considered for similar applications. The modeling done for this study may be extended to account for much greater outlet energy, as well.

Machine Learning Algorithms

Eduard Plett

My objective for summer work in 2011 was to "develop, implement, and test machine learning algorithms for sense-and-avoid systems."

Machine learning algorithms are a subset of artificial intelligence algorithms, which try to modify the behavior of computer-controlled systems based on external inputs from sensors and/or internal inputs from databases.

Machine learning algorithms try to extract relationships between input and output variables and develop a generalized input/output model of the system, which allows correct decision making in the presence of new, incomplete, or inexact inputs.

There are several subsets of machine learning. The 3 major subsets are supervised learning, unsupervised learning, and reinforcement learning. Supervised learning (sometimes called concept finding) is where samples of valid input/output combinations are presented to the agent (learner), which allows it to develop an approximate input/output function. Unsupervised learning, heavily used in data mining, attempts to uncover similarities in data sets and attempts to group or cluster the data according to some criteria. Lastly, reinforcement learning is where, instead of input/output samples, a reward parameter associated with state/action pairs gives the agent an indicator of how closely the actual output matches the desired output.

Unlike the first 2 subsets of machine learning, reinforcement learning algorithms are very well suited for on-line applications as the agent can collect information about the environment by interacting with it, and modify its behavior based on the new information. Therefore, I chose to research reinforcement learning algorithms for the sense-and-avoid systems.
Of the many reinforcement algorithms, I chose the Q-learning algorithm as the most promising. The Q-algorithm assigns a value (the Q-value) to each state/action pair based on immediate and future rewards. The agent is trained to choose an action with the highest Q-value as the optimal action. As mentioned before, it is an online algorithm in that, if the action turns out not to be optimal, the Q-values are modified accordingly.

First, I wrote the Q-algorithm to work in a fixed 7x7 grid, with a start point, a goal point, and an obstacle point. The state was determined from the coordinates of the agent (state 1 through state 49). The allowable actions were "up", "down", "left" and "right", and the reward was given as follows: 100 points if the goal was reached, -100 if the obstacle was hit, and zero (0) for all other positions.

I let the algorithm run (trained the agent) for 1000 iterations, then I tested the agent with various combinations of start, goal, and obstacle points. The algorithm worked flawlessly: the agent was able to navigate even complex mazes (please see figure 1 and figure 2).

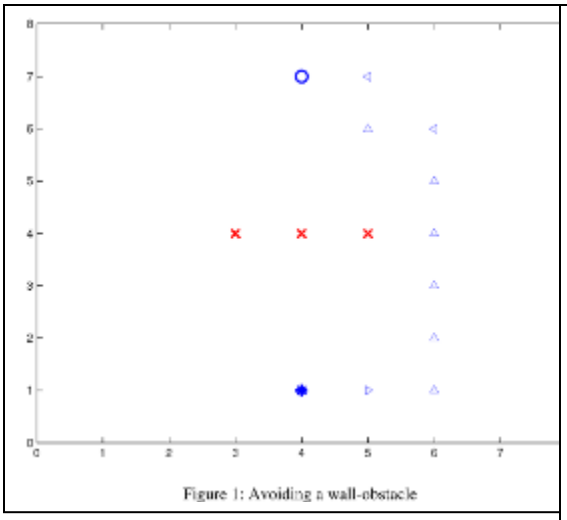

Figure 1: Avoiding a wall-obstacle

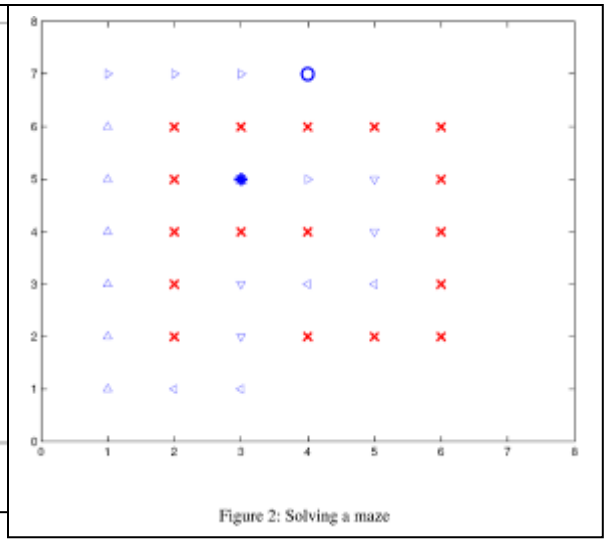

Figure 2: Solving a maze

The grid-based reinforcement algorithm performed well in a simulation, but to make it work in practice there were several modifications that needed to be made. The most important was the reduction of the number of states. Even for a 7x7 grid, 49 states were required. To expand it to a more practical 500x500 grid, 250,000 states would have been required-far too many to perform meaningful training. In addition, the behavior of the agent needed to be independent of the absolute position; only the relative position to the goal and to the obstacle needed to be considered.

After some research, consultation with other faculty, and experimentation, I decided to move away from determining the state of the agent by the position of the agent. Instead, I decided to use the distances to the goal and obstacle, discretizing them using thresholds, and then assigning states based on a combination of goal and obstacle distances. Instead of moving up/down, right/left, the actions were now simply "closer to goal", "away from goal", and "on a tangent" (90º to the obstacle distance vector). I called the resulting algorithm a "grid-free reinforcement learning algorithm" (GFRLA).

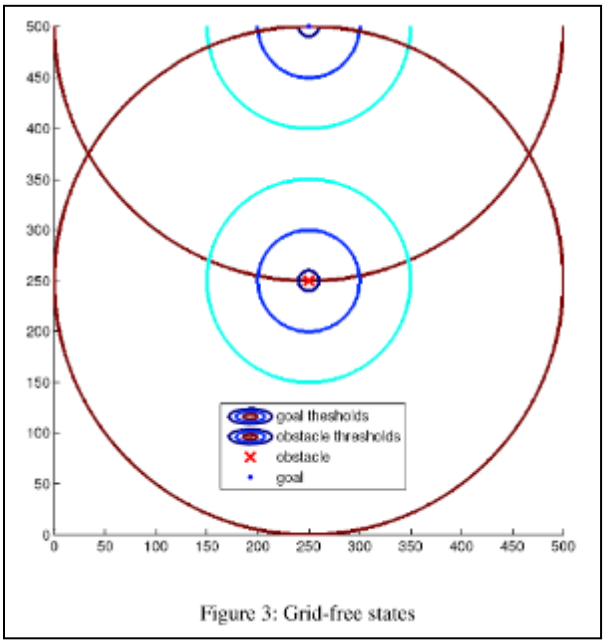

Figure 3: Grid-free states

The algorithm performed satisfactorily if the position of the parameters were close to the training parameters; however, it performed poorly if the position of the obstacle, the start position, or the goal position were moved, or if multiple obstacles were introduced (please see figures 4 - 7).

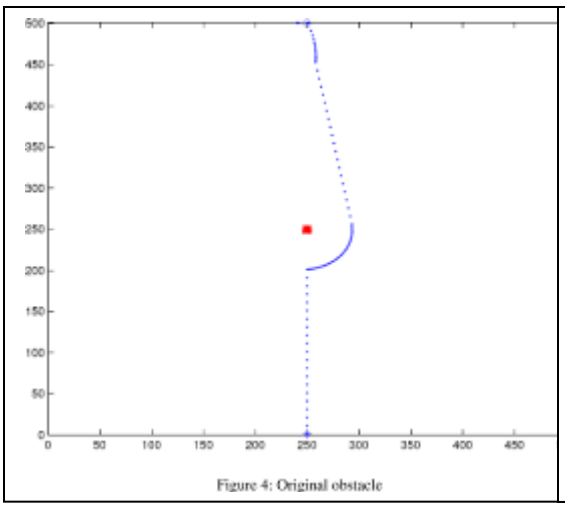

Figure 4: Original obstacle

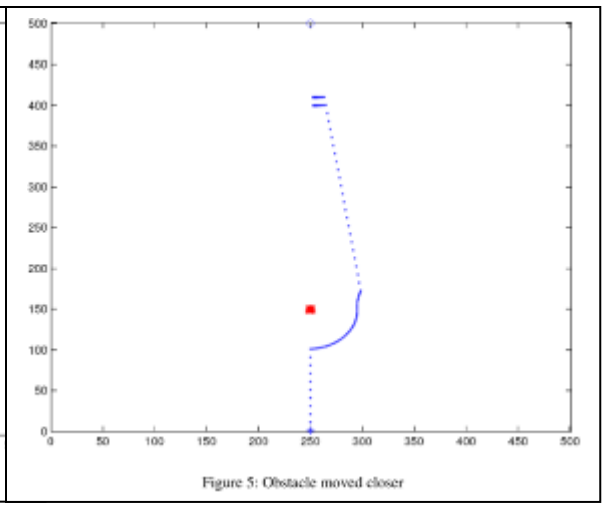

Figure 5: Obstacle moved closer

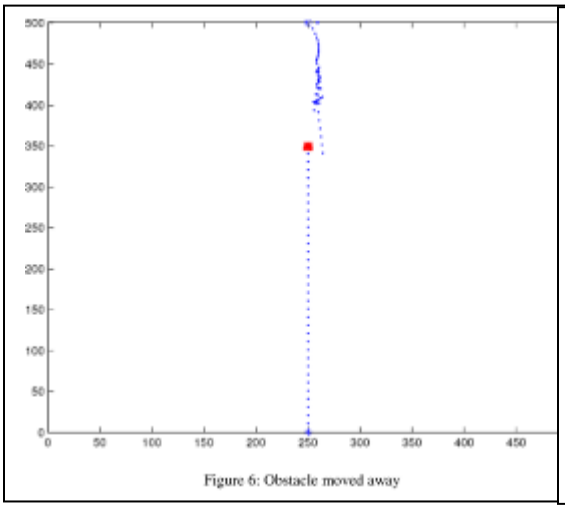

Figure 6: Obstacle moved away

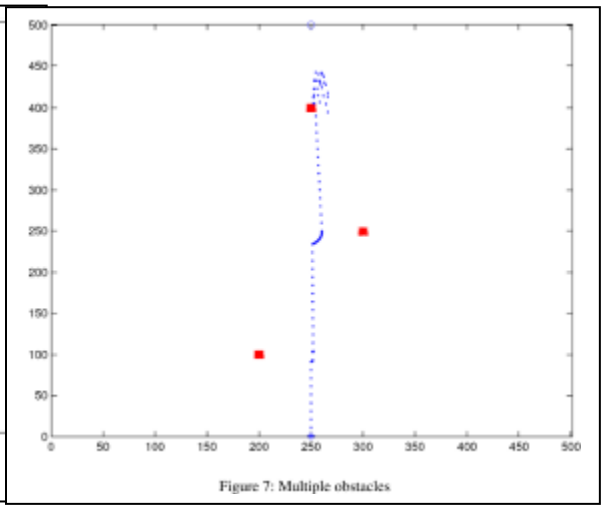

Figure 7: Multiple obstacles

After extensive debugging it became clear that both the method of assigning states, and the method of performing actions, were flawed. First, depending on the thresholds, some states were never entered. Second, some states did not have a distinct policy to enable meaningful training. For example, being in state 24 in front of the obstacle required an "on tangent" action, while being in the same state but behind the obstacle required a "closer to goal" action. Thirdly, the action "away from obstacle" resulted in a dead end if the obstacle and the goal were in a line, since moving away from the obstacle resulted in being placed in a state which required moving closer to goal, shuffling the agent back and forth between those 2 states. Lastly, having a single "on tangent" action proved to be insufficient, as in some states it was preferable to evade to the left, while in others it was preferable to evade to the right, depending on the position of the goal and the position of the obstacle.

After extensive experimentation, I reduced the number of states to eliminate empty and/or ambiguous states, added a 3rd parameter (in front or behind the obstacle), eliminated the "away from obstacle" action; instead added "evade left" and "evade right" actions. As before, I used a single obstacle to train the agent, and then changed the

simulation parameters to determine if the agent performed satisfactorily in different environments. Figures 8 to 14 show the resulting trajectories.

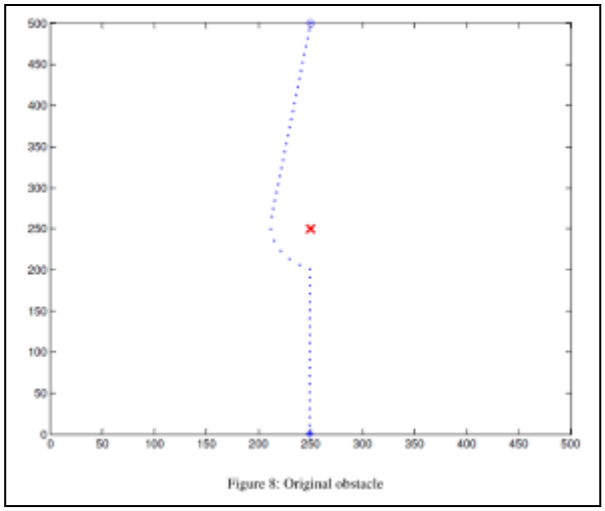

Figure 8: Original obstacle

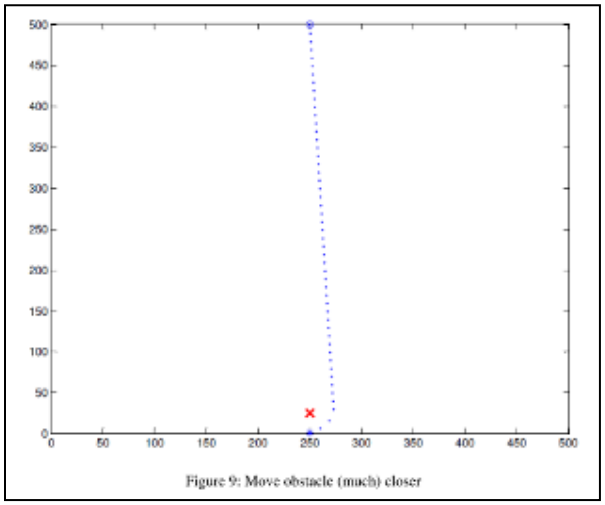

Figure 9: Move obstacle (much) closer

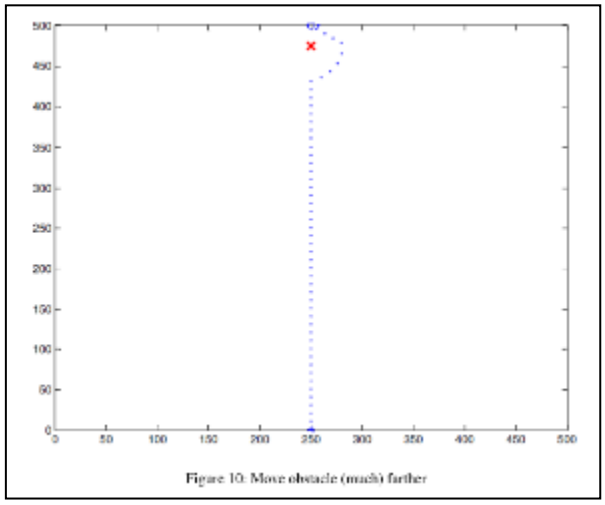

Figure 10: Move obstacle (much) farther

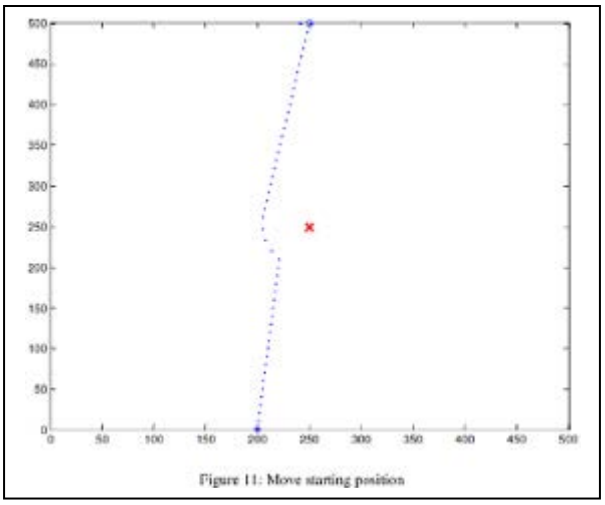

Figure 11: Move starting position

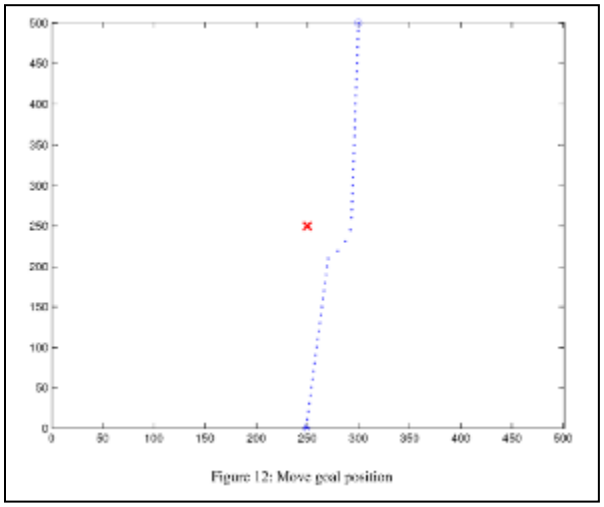

Figure 12: Move goal position

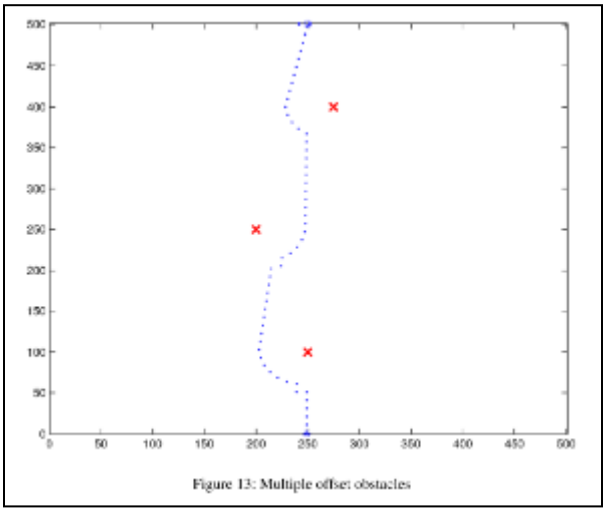

Figure 13: Multiple offset obstacles

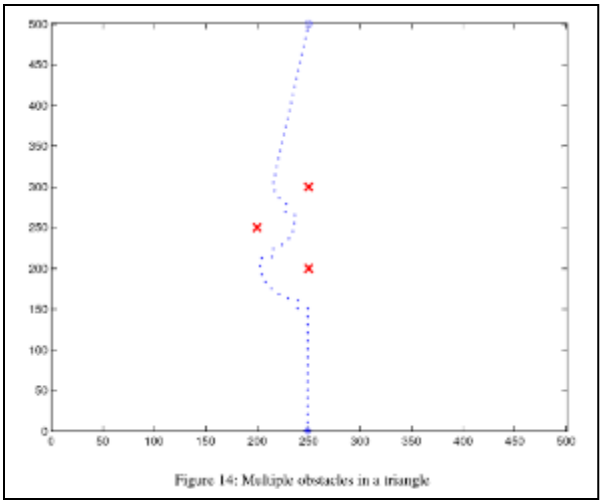

Figure 14: Multiple obstacles in a triangle

As can be seen from the sample figures (I have quite a few more on file), the newest grid-free reinforcement learning algorithm (GFRLA) performed flawlessly in all environments that it was subjected to. However, multiple improvements to the algorithm can be made in the future.

The first improvement is related to the dominant direction of travel. Currently, the goal is always in the +y direction (up) from the starting position. Part of the state-finding algorithm (i.e. the "in-front", "behind", "left", or "right" classification) will need to be modified if the goal is in any other direction.
Secondly, the action repertoire might need to be modified to enable smoother trajectories.
Thirdly, the algorithm might need a mechanism to escape a trap, e.g. when the obstacle has a concave form.
Fourthly, the algorithm needs to be expanded into 3 dimensions for implementation on a UAV.
Fifthly, the algorithm needs to be adapted and tested with a UGV and/or UAV simulator.
Lastly, the algorithm needs to be adapted and tested with a real UGV and/or UAV.
I plan to tackle all of these improvements during the summer of 2012.

Thermal Management Systems for UAV Platforms

Raju Dandu

Unmanned Aerial Vehicle systems are seeing increasing use in civil applications, and the reliability of communication systems is of primary importance. In that aspect, my work is focused on studying the thermal management of RF amplifiers used in wireless communications. The project work involves review and selection of software packages used for modeling and simulation of thermal management systems. After selecting the software, analyze the thermal management issues and best alternatives to dissipate heat from power amplifiers to maximize its reliability and minimize premature failure.

A review of several software options resulted in the selection of COMSOL Multiphysics engineering software. The software will be used to analyze different cooling techniques and thermal interface materials.

As a next step, trends in electronics cooling were explored to identify the current issues related to thermal management of electronics. Recent trends in unmanned aerial vehicles indicated the need for more capable and efficient power and thermal management systems. A number of requirements in electronics are unique to UAV systems compared to the regular aviation. Rising heat density in electronics exposed to a range of normal to harsh environments, coupled with size, weight and power (SWaP) constraints, has forced consideration of alternative cooling solutions from a platform perspective. This led to solutions utilizing cooling products that provide excellent environmental isolation in small form factors for a broad range of power densities. Several electronics options, enclosure alternatives, and environmental conditioning solutions are available today.

There are several platform level approaches to electronics cooling, the most common are air-cooled, conduction-cooled, and liquid-cooled subsystems -including Spray Cool's direct-spray approach. Current cooling techniques used at the component level, such as using better materials or heat spreading, are addressing the issue locally. The issue still remains to get the heat out of the system and off the vehicle. Further, the integration of commercial off the shelf components adds complexity to thermal management. The study revealed that systems designers must address three basic issues in thermal management for military electronics applications: high enough thermal conductivity to dissipate heat, a low coefficient of thermal expansion to reduce thermal stresses and solder attachments, and low-density thermal interface materials (TIM).

Therefore, using COMSOL software, it is necessary to evaluate not only the cooling techniques, but also the low density thermal interface materials. Further, it is necessary to experimentally study forced air cooling coupled with different thermal interface materials to address thermal management issues of UAV platforms.

Archival Publications (published) during reporting period: None

Changes in research objectives, if any: None

Change in AFOSR program manager, if any: None

Extensions granted or milestones slipped, if any: None

Include any new discoveries, inventions, or patent disclosures during this reporting period (if none, report none): As described.